kingdom Saudi Arabia

Al-imam Mohammad Ibn

Saud Islamic University

College of Department of Chemistry

المملكة العربية السعودية

جامعة الإمام محمد بن سعود الإسلامية

كلية العلوم

قسم الكيمياء

Fabrication nano composite based on graphitize carbon nitride and its derivative

A graduation research submitted by:

Fay Thamir Al-dossari 434026577

Amjad Mohammed Al-bareh 442014075

Ghaliah Refaei Al-otaibi 441020007

Amal Abdulaziz Al-ghamdi 440018979

Under supervision:

Dr.Laila Alqarni

Second semester, February 2025

Acknowledgment

We are profoundly thankful for the countless blessings and grace from Allah. Our heartfelt gratitude goes out to Imam Muhammad Bin Saud Islamic University for their invaluable support. We extend our sincere appreciation to Dr. laila saad Al-Qurni, who not only proposed and organized this project but also provided us with guidance, encouragement, and the essential skills for conducting research responsibly and confidently. Our special thanks

are reserved for our parents and other family members whose unwavering support, encouragement, well-wishes, and prayers have been a driving force behind our accomplishments. Without their support, we would not have achieved what we have today

Abstract:

This project aims to develop and manufacture an innovative nanomaterial with distinctive properties that enhance its efficiency in various applications. The goal was synthesis nanocomposite based on graphitize carbon nitride and its derivative, while studying its physical and chemical properties using advanced analysis techniques such as SEM, EDX, FTIR, UV-Vis. This research contributes to enhancing our understanding of nanomaterials and the possibilities of improving their properties through structural and surface modifications, which opens new horizons for their use in advanced technical and environmental applications. Based on current nanocomposite, it is recommended to conduct future studies to apply it as adsorbent in water treatment or other applications.

الملخص

يهدف هذا المشروع إلى تطوير وتصنيع مادة نانوية مبتكرة ذات خصائص مميزة تعزز كفاءتها في تطبيقات مختلفة. وكان الهدف هو تصنيع مركب نانوي قائم على نيتريد الكربون الجرافيتي ومشتقاته، مع دراسة خصائصه الفيزيائية والكيميائية باستخدام تقنيات التحليل المتقدمة مثل المجهر الإلكتروني الماسح، EDX، FTIR، UV-Vis. يساهم هذا البحث في تعزيز فهمنا للمواد النانوية وإمكانيات تحسين خصائصها من خلال التعديلات البنيوية والسطحية، مما يفتح آفاقًا جديدة لاستخدامها في التطبيقات التقنية والبيئية المتقدمة. بناءً على المركب النانوي الحالي، يوصى بإجراء دراسات مستقبلية لتطبيقه كمادة ماصة في معالجة المياه أو تطبيقات أخرى.

Contents:

Figures:

Figure1:	graphitic carbon nitride; ; metal oxide; photocatalysts; sensors; bacterial disinfection; supercapacitors
Figure2:	Overview of commonly used nanoparticle (NP) types, classified as organic, inorganic, or composite structures
Figure3:	Schematic diagram for biological synthesis of Ag NPs
Figure4:	a, b) SEM for the cuurent nancompositie showing the different deposited nanoparticles (c) Scanning electron microscopy image after analysis(Image J) showing the porisity in the nanocomposite.
Figure5:	(a) EDX for the nanocomposite showing the elemental analysis,(b) Mapping Analysis of nanocomposite
Figure6:	Decoration of NPs to Fabrication of $Ag@Fe_2O_3.CuO@g-C_3N_4$
Figure7:	(UV-Vis) Analysis of Nanocomposite
Figure8:	Fourier-Transform Infrared spectroscopy (FTIR) Analysis of nanocomposite .
Figure 9	The band gap energies of the nanoparticles CuO, Fe_2O_3, AgNps, ,G-C_3N_4 and the nanocomposite.

Chapter I

1.Introduction

1.1. Graphitic carbon nitride ($g - C_3N_4$)

Graphitic carbon nitride ($g - C_3N_4$), a polymeric semiconductor, has garnered a lot of attention lately in the hunt for reliable and stable VLD semiconductor photocatalysts. Metal-free $g - C_3N_4$ has several advantages due to its heptazine ring structure and high condensation degree, including strong physicochemical stability, an attractive electronic structure [1]. graphitic carbon nitride ($g - C_3N_4$) is also a polymeric visible-light-active photocatalyst with a bandgap around 2.7 eV (460 nm)[2]. Because of its easy, inexpensive, and eco-friendly method of preparation, as well as its promising stability and strong physicochemical qualities for usage in a variety of applications, $g - C_3N_4$ has grown in importance in the fields of chemistry, physics, and engineering[3] . In contrast to other semiconductors, $g - C_3N_4$ is easily synthesized using a variety of techniques, has great thermal stability up to 600 °C in air, and favorable electrical topologies and morphologies[5 ,4]. $g - C_3N_4$ is a viable option for visible light photocatalytic applications using solar energy because of these special characteristics. Also, one-step polymerization of inexpensive feedstocks such as cyanamide, urea, thiourea, melamine , and dicyandiamide yields $g - C_3N_4$ in large quantities and with ease. However, pure $g - C_3N_4$ has drawbacks such low visible light usage efficiency, small specific surface area, and quick recombination of photogenerated electron-hole pairs.

One of the most significant renewable clean energy sources is solar fuels, and photocatalytic conversion of CO_2 into the valuable hydrocarbon fuel (CH_4) is seen as a difficult but promising use of sustainable energy sources [6].

with enhanced physicochemical characteristics and high photocatalytic activity is becoming more and more necessary. Due to its distinct two-dimensional layered structure, the $g - C_3N_4$ is well suited for hybridization with other elements. Recently, a number of strategies have been used to improve $g - C_3N_4$'s visible light photocatalytic performance[6].

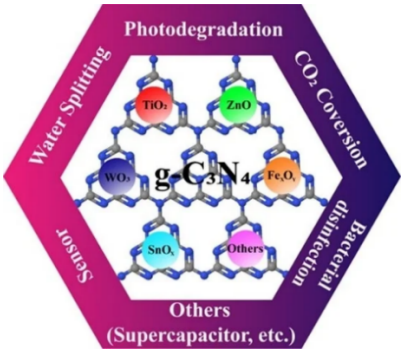

Figure 1. graphitic carbon nitride; $g - C_3N_4$; metal oxide; photocatalysts; sensors; bacterial disinfection; supercapacitors [7].

1.2 Nano particles.

Nanoparticles (NPs) are materials with at least one dimension under 100 nm, encompassing a broad variety of materials. They are generated through nanotechnology processes. Nanoparticles can be categorized into four groups based on their shapes and the number of dimensions outside the nanometric scale: 0D, 1D, 2D, or 3D. 0D materials have no dimensions outside the nanometric range, 1D materials have one dimension outside the nanometric range, 2D materials have two dimensions outside the nanometric range, and 3D materials have three dimensions outside the nanometric range [8].

Using 20-nm silver (Ag), gold (Au), palladium (Pd), and platinum (Pt) nanoparticles, researchers have identified the importance of nanoparticles, such as their optical qualities, and discovered that a substance's physiochemical properties can be modified by volume. Size and shape impacts and unique colors have been discovered. This resource has been found to be beneficial in bioimaging [9].

Nanoparticles are made up of three layers: the core, which is the central part of the NP; the surface layer, which surrounds the core; and the environment surface. Essentially, nanoparticles are not molecular elements in and of themselves. [10] Due to the exceptional features of NPs, experts from various fields are interested in these products. NPs can be used for a variety of purposes, including drug delivery [11], gas detection [12-14], chemical and biological detection [15], CO_2 capture [16, 17], and more [18].

Characterization of nanoparticles involves different methods to analyze their chemical and physical properties. These techniques include X-ray photoelectron spectroscopy

(XPS), scanning electron microscopy (SEM), transmission electron microscopy (TEM), X-ray diffraction (XRD), particle size analysis, ultraviolet (UV) spectroscopy, and infrared (IR) spectroscopy [19].

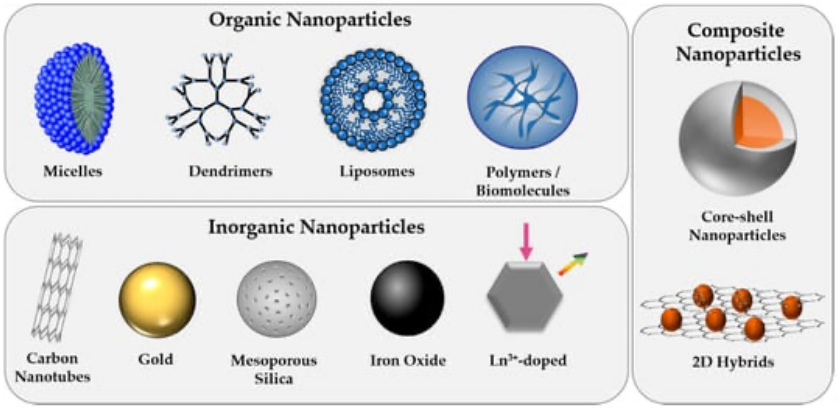

Figure 2. Overview of commonly used nanoparticle (NP) types, classified as organic, inorganic, or composite structures [20].

1.2.1. Iron oxide nanoparticles (α-Fe_2O_3 NPs)

Iron oxide nanoparticles (α-Fe_2O_3) have unique features that make them an important field in modern scientific research [21] . Its compound can be identified by its red colour and rhombohedral crystal shape. Hematite, one of the most stable forms of iron oxide, has excellent corrosion resistance, making it ideal for environmental and technical applications [22]. Hematite's magnetic characteristics depend on its size, shape, and inter-particle interactions, ranging from antiferromagnetic to weakly ferromagnetic and superparamagnetic. Hematite also has a hardness range of 5.5 to 6.5 on the Mohs scale and semi-conducting characteristics with a band gap of 2.1 eV. [22].

Iron oxide nanoparticles are useful in imaging and medication targeting due to their magnetic properties. These nanoparticles have showed potential in treating diseases such as cancer by improving the delivery and efficacy of therapeutic agents [23]. They are also used in water treatment to remove pollutants including colours and heavy metals, with excellent efficacy in eliminating malachite green dye from aqueous solutions [24]. Hematite is employed industrially as a pigment, catalyst, and electrode material , according to its stability and non-toxicity [22].

The biocompatibility and therapeutic potential of iron oxide nanoparticles have also been the subject of research. They can cause apoptosis in cancer cells and are used to treat cancer through hyperthermia. Furthermore, their use as contrast agents in magnetic resonance imaging (MRI) emphasizes their important role in non-invasive medical diagnostics . Iron oxide nanoparticles' adaptability and multipurpose nature continue to motivate research and development across a range of scientific and industrial domains[23].

1.2.2. Silver Nanoparticles (Ag NPs)

MNPs offer unique characteristics that make them more appealing to society, particularly Ag NPs. The primary focus of research has been on the unique physical, chemical, and biological characteristics of Ag NPs. The main cause of their widespread use is the discrepancy between the bulk structure and Ag NPs' form, composition, crystallinity, and structure[25]. There are numerous uses for Ag NPs in biological domains because of their size-dependent optical and catalytic properties. Because Ag NPs are impervious to human skin, They have been used as safe stabilizers in a range of cosmetic products in factories [26]. These molecules have received a lot of interest, as evidenced by the figures displaying the needs and expenses in Ag NP-related research. The market for Ag NPs has been steadily growing over the last 15 years, with an estimated yearly production of more than 500 tons of NPs to satisfy the needs of various industries[27]. According to reports, Ag NPs' catalytic, physical, and optical abilities are significantly influenced by their size, distribution, morphological shape, and surface features. Their unique properties allowed the silver nanoparticle to be applicable in many applications, as showing in Figure 3.

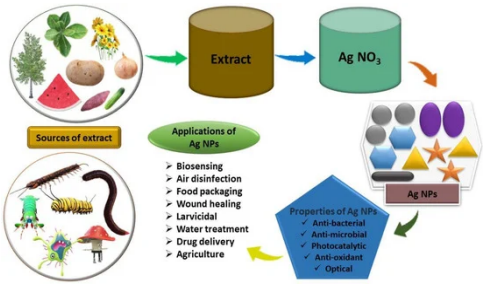

Figure 3. Schematic diagram for biological synthesis of Ag NPs[28].

1.2.3. Copper oxide nanoparticles (CuO (NPs)

The synthesis process determines the CuO NPs' properties, which are crucial for their uses in various fields, including the most common, biomedical research. Since it enables customized modeling of the nanoparticles' optical, catalytic, electrical, and biological capabilities, their size—which may be modified during synthesis, is their most crucial characteristic [28]. According to these investigations[29]. According to these investigations[30], the particle size may impact the magnetic properties of CuO NPs. Still, other factors, such as the synthesis process, bulk material composition and ratio, and other physico-chemical characteristics, undoubtedly also govern these qualities.

CuO Nanoparticle Toxicity When evaluated on mammalian cells and on different animal models, CuO nanoparticles exhibit various hazardous effects both in vitro and in vivo [31, 32]. According to a 1995 study, copper's bioavailability is the main determinant of its toxicity, which is comparable to what occurs with hazardous heavy metals [33]. The following characteristics can be changed to affect CuO NPs' toxicity: (a) Size: Compared to bigger nanoparticles, smaller ones are more hazardous. (b) Surface charge: a positive charge increases the toxicity of nanoparticles. This positive charge facilitates interactions between cells and nanoparticles. (c) Dissolution: The solution's temperature and pH significantly impact the dissolution of CuO NPs.

Applications Metal oxide nanoparticles have garnered particular attention due to their extensive use as chemical sensing devices, industrial catalysts, disinfectants, antimicrobials, fillers, opacifiers, semiconductors, and in the development of cosmetics and microelectronics [29, 34-37] .

CHAPTER II

Experimental part

2. 1 Chemicals and Materials:

2.1.1 Material

Material of Ag: Silver nitrate ($AgNO_3$) (0.1M), Sodium acetate (2M)

Material of CuO: Copper chloride ($CuCl_2$)(0.1),$NaOH$(0.1M)

Material ofFe_2O_3: $FeSO_4.7H_2O$ (ferrous sulfate heptahysrate) (20 g) ,NaOH (1M) (drops) , Deionized water (200 ml) ,Distilled water

2.1.2 Characterization

The tool used include several commonly used laboratory glassware, model oven, electric furnace, dry oven, Balance, thermometers, clamps, centrifuge, magnets, pellets, hot plates (stir and heat), Scanning Electron Microscopy (SEM) , The JEOL JSM-7610F Scanning Electron Microscope (SEM) is an advanced instrument designed for high-resolution imaging and analysis of nanoscale samples. It offers a magnification power of up to 1,000,000 times (1,000,000X), with a resolution of 1 nanometer (nm), allowing for the visualization of extremely fine details. The device operates with an electrical current ranging from 5 to 15 kV, with 15 kV being the typical operating voltage. This microscope is widely used for examining both biological samples, such as cells and tissues, and non-biological materials, such as engineered substances or solid objects. One of its key features is the built-in X-ray capability, which allows for the identification and analysis of the chemical elements present in a sample. The JEOL JSM-7610F is an essential tool in scientific research and various industrial applications that require precise nanoscale analysis.

UV-visible spectroscopy model: UV-Vis diffuse reflectance spectra (DRS) were recorded using BaSO4 as a 200-800 nm standard using the Shimadzu UV-Vis spectrophotometer (2600i UV-Vis, Japan). For Fourier Transform Infrared (FTIR) model, The materials' infrared spectra were captured on a German-made Brucker-FTIR (Vector 22) with a KBr pellet. Using a JDX:8030 X-Ray, JEOL, manufactured in Japan, X-ray diffraction (XRD) was used to identify the crystalline phases for all samples under investigation. Cu-filtered CuKa radiation (A 2' 1.5418A) energised at 45 kV and

10 mA was used to run the patterns. The samples were studied between 28 = 10 and 80º at room temperature .

The materials' infrared spectra were captured on a German-made Brucker-FTIR (Vector 22) with a KBr pellet. UV-Vis diffuse reflectance spectra (DRS) were recorded using $BaSO_4$ as a 200-800 nm standard using the Shimadzu UV-Vis spectrophotometer (2600i UV-Vis, Japan).

2.2 SYNTHESI OF NANOPARTICLES:

2.2.1. Synthesis of Fe_2O_3 Nanoparticles by Precipitation Method

α-Fe_2O_3 nanoparticles were synthesized using the precipitation method. Initially, 20 g of ferrous sulfate heptahydrate ($FeSO_4 \cdot 7H_2O$) were dissolved in 200 mL of deionized water under continuous stirring. A sodium hydroxide (NaOH) solution (1.0 mol/L) was added dropwise to the solution until the pH reached approximately 14. The mixture was stirred for a few minutes, leading to the production of a black precipitate of iron hydroxide nanoparticles ($Fe(OH)_2$ NPs). The precipitate was collected and thoroughly washed with distilled water several times until the pH of the wash water was neutral (pH ≈ 7). The black precipitate was then dried at 80 °C for 16 hours in a drying oven. Finally, the dried precipitate was heated at 600 °C for six hours to complete the synthesis, in a muffle furnace, yielding iron oxide nanoparticles (α-Fe_2O_3 NPs) [38].

2.2.2. Synthesis of silver Nanoparticles AgNPs(Chemical reduction method

Silver colloid have been prepared using the chemical reduction method, Which depend on reducing silver nitrate ($AgNO_3$) by sodium acetate. After preparing 500ml of stock solution of silver nitrate, 500ml of stock solution(0.1M)of silver nitrite was taken and add to the beaker ,the solution has heated temperature of 100 °C .Covered with glass on a hot plate, stir the solution with magnetic stir bar .Once boiling, add 5ml of sodium acetate (2M) dropwise , About one drop per second, wait for the solution to change to light silver color . Carefully remove the beaker from the hot plate and let the solution cool at room temperature [39].

2.2.3. Synthesis CuO Nanoparticle (precipitation method):

Copper chloride ($CuCl_2$) was used in the precipitation process to create CuO nanostructures. To get a 0.1 M concentration, the precursor was first dissolved in 100 milliliters of deionized water. Then we added 0.1 M NaOH solution gradually while vigorously stirring until the pH reached 14. The black precipitates will appear after we wash with deionized water, and 100% ethanol repeatedly until the pH reaches 7. After obtaining black precipitates, deionized water and 100% ethanol were used to wash the precipitates multiple times until the pH reached 7. The cleaned precipitates were then dried for 16 hours at 80 °C. Lastly, the precursors underwent a 4-hour calcination at 500 °C[40]

2.2.4. Synthesis of Graphitic carbon nitride g-C_3N_4 Preparation

The production of g-C_3N_4 nanomaterial was achieved through the thermal decomposition of urea molecules. A total of 3.5 g of urea material was subjected to incineration at a temperature of 550 ◦C for a duration of 120 min . The unprocessed g-C_3N_4 nanomaterials, which had a yellow color, were subsequently subjected to cooling, grinding, and packaging processes and placed into dark containers[41].

2.2.5. Fabrication of Ag@Fe_2O_3.CuO@G-C_3N_4 Preparation

In this procedure 30 mL of alcohol was added to a beaker. To achieve complete dispersion of the G-C_3N_4, the material was introduced into the alcohol and stirred for 10 minutes. Following this, nanoparticles were added to the solution, and the mixture was stirred continuously for an additional hour to ensure the formation of a homogeneous suspension. To remove residual solvents, the suspension was transferred to an oven and dried at 90°C. Once the nanoparticles were completely dried, the sample was subjected to a thermal treatment at 600°C for two hours. Finally, the resulting material was ground to a fine powder to facilitate the intended chemical reaction and product formation.

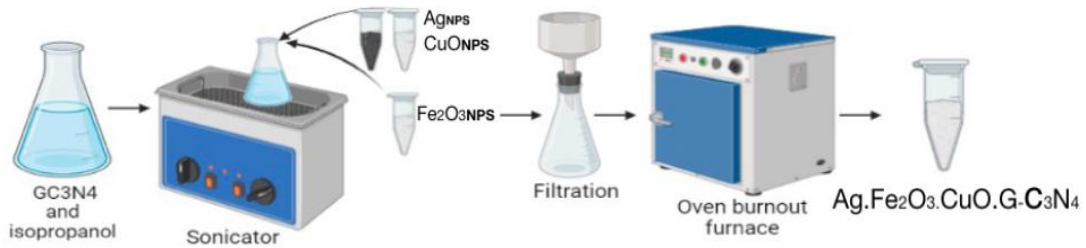

Figure 4: Decoration of NPS to Fabrication of Ag.Fe_2O_3.CuO.g-C_3N_4

Chapter III

Results and Discussion

3.1.1 SEM, EDX, Mapping Analysis of $Ag@Fe_2O_3.CuO$@ g-C_3N_4 nanocomposite):

The SEM image of the nanocomposite sample, featuring nanoparticle structures and Ag@Fe_2O_3.CuO@g-C_3N_4 from the SEM pictures in Figs (5), it can be noted that Ag and Fe_2O_3 nanoparticles are randomly dispersed. The SEM results demonstrate that the annealed nanocomposites are comparatively porous and heavily agglomerated with the nano entities and exhibit distinct pores within the sheets in different sizes. Moreover, Ag@$Fe_2O_3.CuO@g-C_3N_4$ nanocomposite showing in the shape of ovals and rods. The EDX map in Figure (10) results revealed the presence of Oxygen (O), Carbone (C), copper (Cu),Carbon (C),Iron(Fe),Nitrogen (N) ,Silver (Ag) .“The detected elements within the sample were identified, and the analysis revealed spectral peaks corresponding to the generated nanoparticles.”optical absorption characteristics.

During the synthesis process, nanoparticles of iron oxide, silver and copper oxide were formed, which were deposited on graphite carbon nitride sheet. scanning electron microscopy images of the lyophilized silver nanoparticles primarily revealed spherical particles less than 100 nm. SEM analysis of the nanoparticles was therefore carried [1]. Samples are structured like sheets. When compared to bulk g-C_3N_4, the porous g-C_3N_4exhibits larger holes or a rougher surface as a result was achieved through the thermal decomposition of urea molecules. This outcome shows that holes were created throughout the synthesis process as result of thermal decomposition of urea molecules [2].At iron oxide nanoparticles appear to be spherical in shape with narrow size

distribution. From the SEM image of the copper oxide nanoparticles, it was observed that the particles were well-distributed spherical, had a well-defined and almost uniform crystal structure[42, 43].

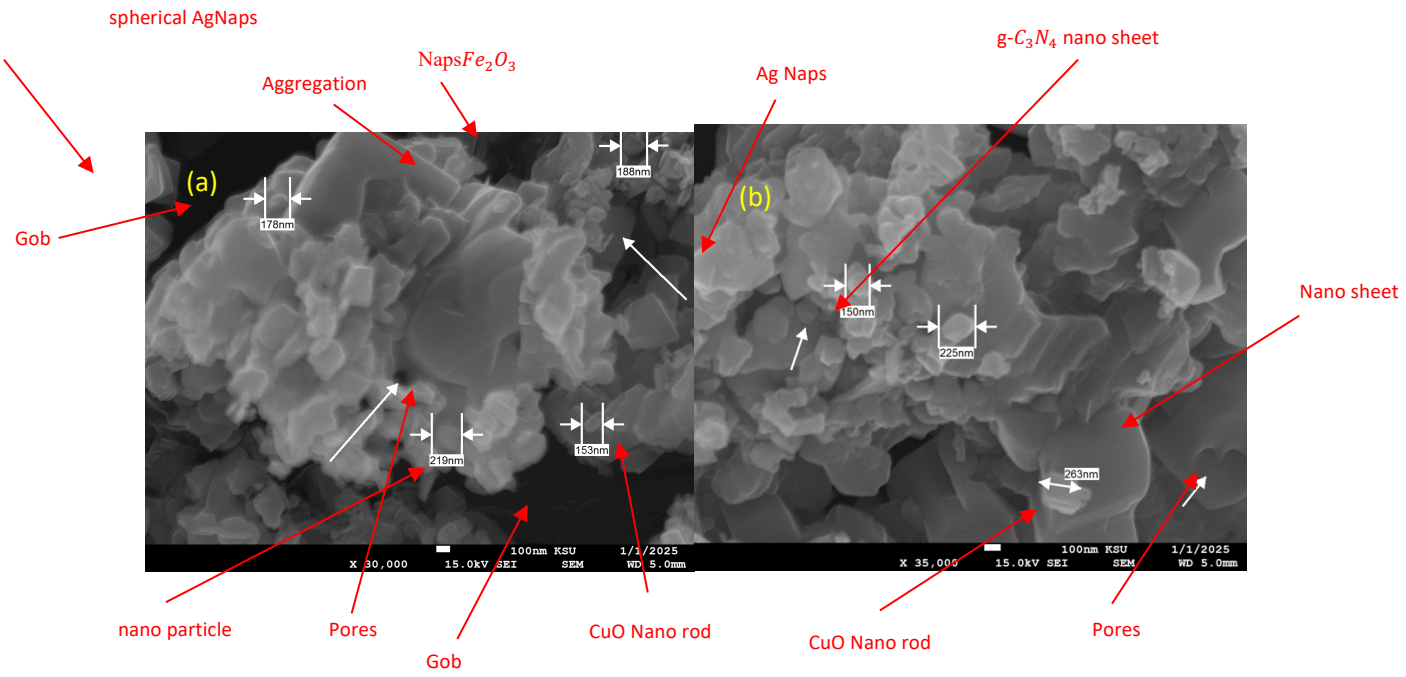

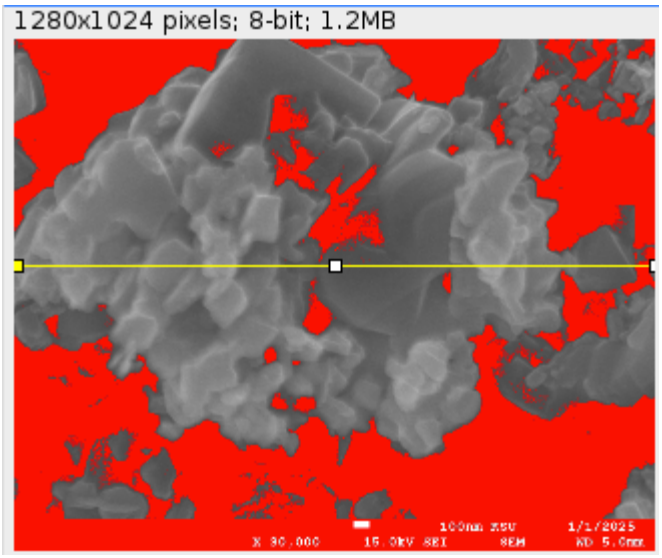

Figure 5 :a, b) SEM for the cuurent nancompositie showing the different deposited nanoparticles (c) Scanning electron microscopy image after analysis(Image J) showing the porisity in the nancomposite.

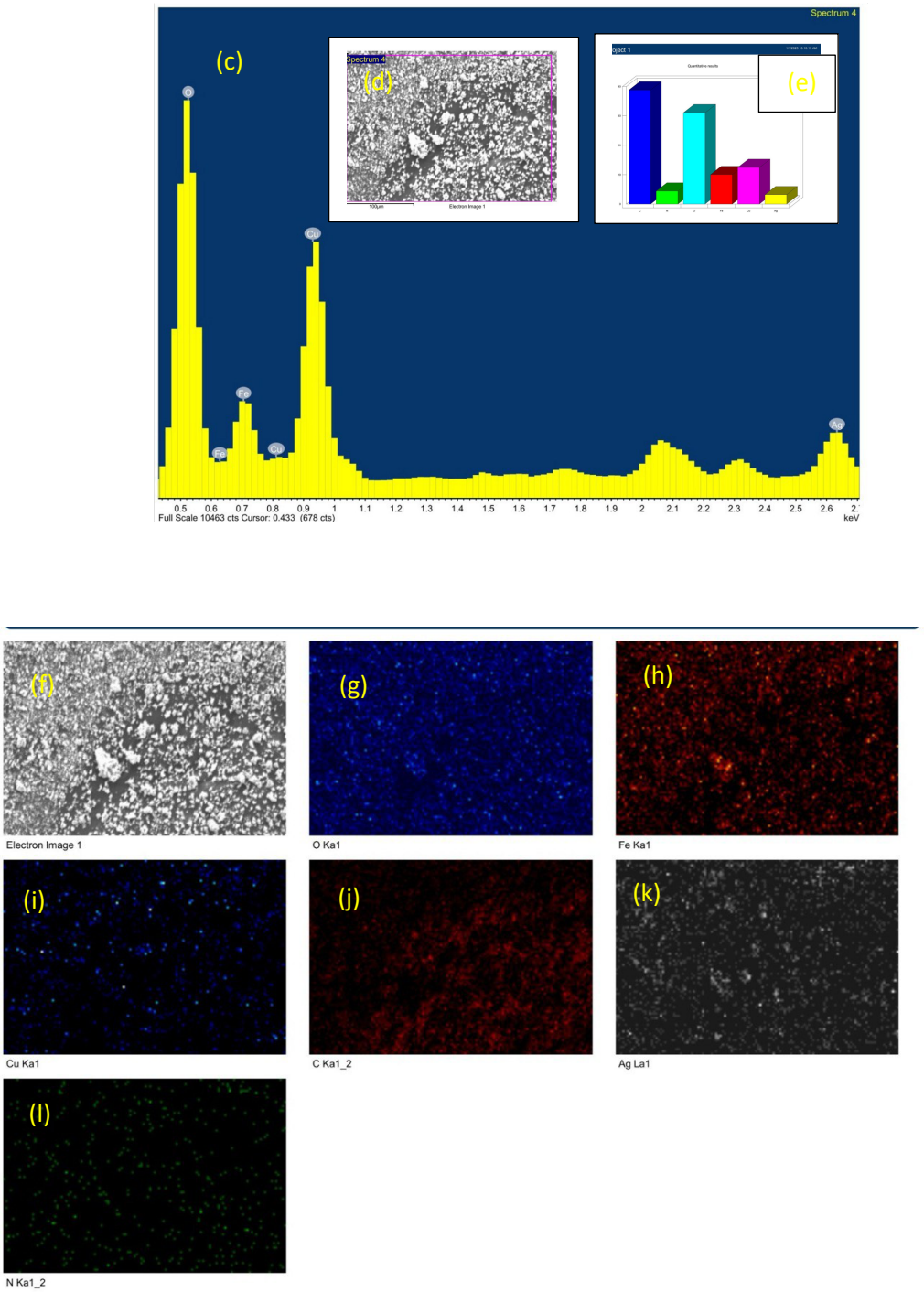

Figure 6: (a) EDX for the nanocomposite showing the elemental analysis, (b) Mapping Analysis of (Ag@Fe_2O_3.CuO@gC_3N_4).

3.1.2 Fourier-Transform Infrared spectroscopy (FTIR) Analysis of Ag@.Fe_2O_3CuO@G.C_3N_4 nanocomposite :

Analytical methods for identifying organic, polymeric, and occasionally inorganic materials include Fourier transform infrared spectroscopy (FTIR spectroscopy) and FTIR analysis. With the FTIR analysis method, chemical characteristics are observed by scanning test samples with infrared light The pristine g-C_3N_4's FTIR spectrum shows wide absorption bands in the 3280–3070 cm^{-1} range, which are attributed to the overlap of the stretching vibration of the N-H structural bands as well as the dampness O The extension of C–N and C-N bonds show up as a series of bands in the range,1650–1230 cm^{-1} centered on the absorption band at 804 $cm^{-1}$is notable for the bending vibration of the s-triazine ring, indicating the prevalence of g-C_3N_4's hexazine units While the g-C3N4 and Ag,Fe_2, CuO are bound together[44].

CuO: the sharp band stretching vibrations, 1040 and 1301 cm^{-1} and 1701cm–1 stretching of the Cu=O bond[45, 46].

GC3N4: spectrum of g-C3N4, the peak at 1650 cm^{-1} and 1850 cm^{-1} stretching

Nanocomposites: The Brod band 1600-1850 cm^{-1}, and 600 cm^{-1}, 950cm^{-1} the stretching vibration of and bending vibration.

Ag: The wed band stretching vibrations [47], 300 cm^{-1} and 1300 cm^{-1}

Fe_2O_3 : the Brod band 630 cm^{-1}to1100 cm^{-1} and 1200 cm-1 to 1500 cm^{-1} stretching.

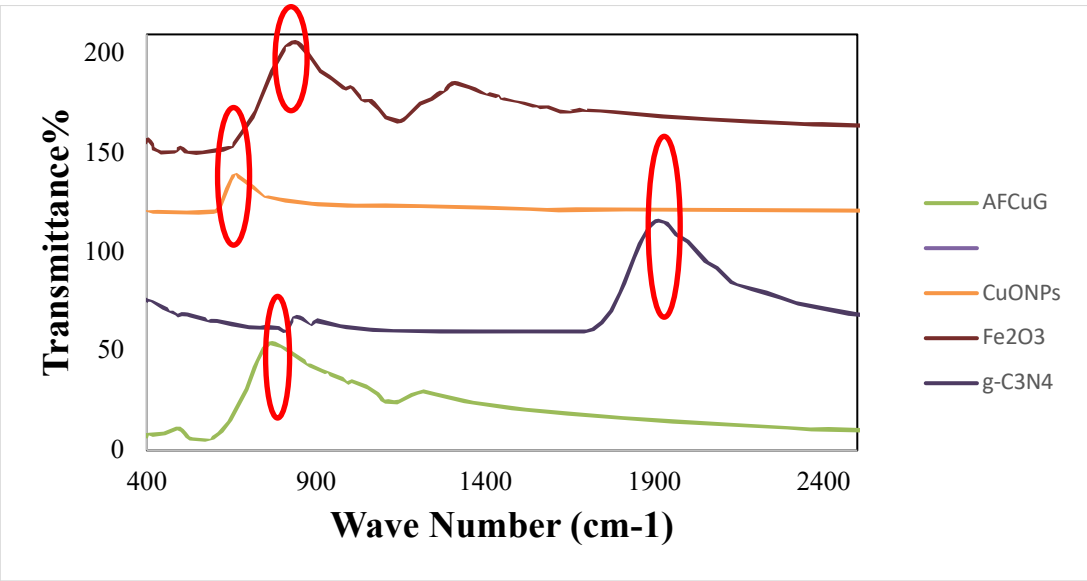

Figure 7: Fourier-Transform Infrared spectroscopy (FTIR) Analysis of $(\mathrm{Ag@}Fe_2O_3.CuO@g-C_3N_4)$

3.1.3 Ultraviolet-Visible Spectroscopy (UV-Vis) Analysis for (Ag.@Fe_2O_3.CuO@G.C_3N_4 nanocomposite):

In analytical chemistry, UV-visible spectroscopy is a widely used and practical instrument. The primary applications of this instrument are in the identification and qualitative analysis of chemical compounds. The features of metallic nanoparticles are greatly influenced by their size and arrangement. When molecules or atoms receive UV radiation, their electrons are stimulated from lower energy levels to higher energy levels. We have collected UV-visible spectra in the wavelength range of 200–800 nm for the current investigation (Fig8.). The large peaks observed at A prominent absorption band is visible in the UV-Vis absorption spectrum of the $g-C_3N_4$NP solution at 560 nm (Figure8). $AgNO_3$ was used to create Ag, and the highest absorbance of the nanosized Silver particles formed via surface plasmon absorption was approximately 220-430 then from 680-740 nm [7].Fe_2O_3 nanoparticles were found in this investigation using the 390-800 nm range. UV-vis absorption spectra are used to study the optical characteristics of $g-C_3N_4$, as illustrated in Fig8.

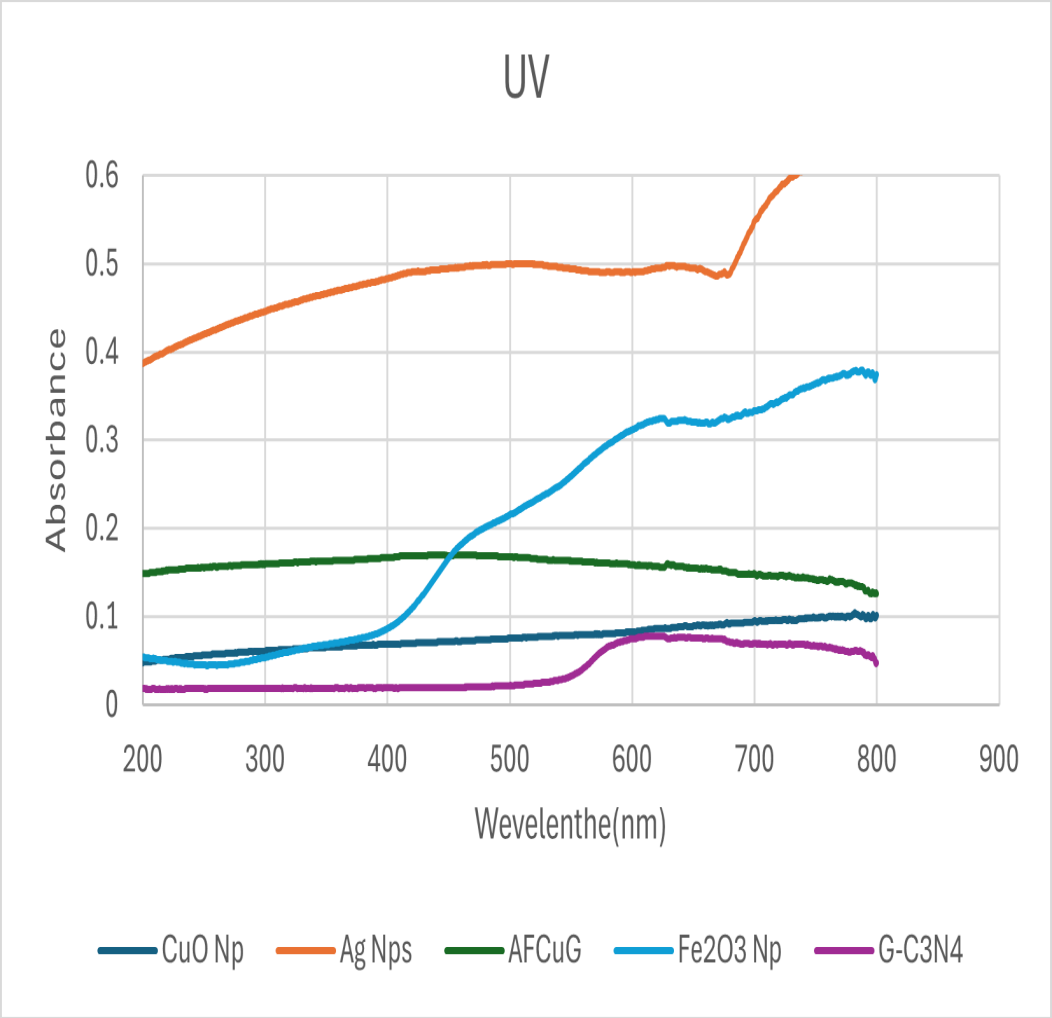

Figure8 : (UV-Vis) Analysis of ($Ag.Fe_2O_3.CuO.g-C_3N_4$) Nanocomposite

Optical properties

UV-visible diffuse reflectance spectroscopy (UV-DRS), which operates in the wavelength range of 200-800 nm, is used to assess the optical properties of pure and composite materials, as illustrated in the figure 9.

In order to apply the Tauc approach, it is assumed that the energy-dependent absorption coefficient α can be represented by the equation (1):

$$(\alpha \cdot h\nu)^{1/\gamma} = B(h\nu - Eg) \qquad (1)$$

where Eg is the band gap energy ,h is the Planck constant, ν is the photon's frequency, and B is a constant. The γ factor is equal to 1/2 for the direct transition band gap and 2 for the indirect transition band gap, depending on the type of electron transition. Diffuse reflectance spectra are typically used to calculate the band gap energy. The Kubelka-Munk function can be used to convert the measured reflectance spectra to the equivalent absorption spectra, according to the hypothesis put forward by P. Kubelka and F. Munk in 1931[48]. (F(R∞), showon in eq 2

$$F(R_\infty) = (1 - R_\infty)^2/2R_\infty \qquad (2)$$

where R_∞ is the reflectance of an infinitely thick specimen, Putting $F(R_\infty)$ instead of α into eq 1 yields the form (3) [49]:

$$(F(R_\infty) \cdot h\nu)^{1/\gamma} = B(h\nu - Eg) \qquad (3)$$

The energy gap values of samples can be determined from $(F(Rw)hv)^2$ vs. hv plot by linear extrapolation of the $(F(Rw)hv)^2$ to zero. The band gap energies of the nanoparticles CuO, Fe_2O_3, AgNps, ,G-C3N4 and the nanocomposite in the current study are 1.2 ev, 3.2 ev, 1.1ev , 2.3ev, 1.35ev.

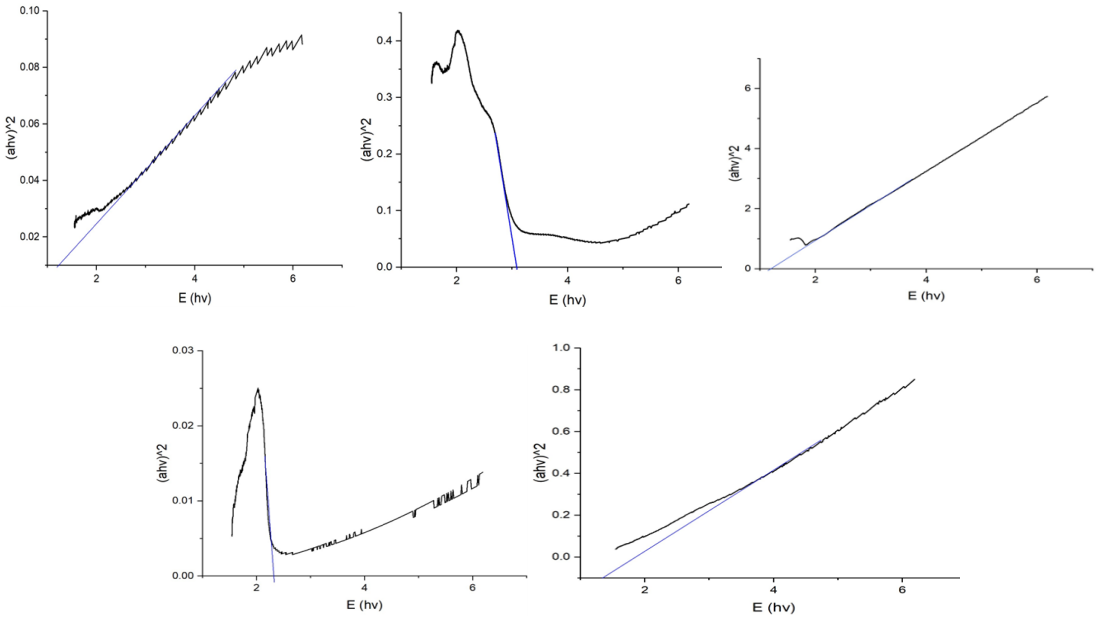

Figure 9: The band gap energies of the nanoparticles CuO, Fe_2O_3, AgNps, G-C_3N_4 and the nanocomposite.

Conclusion:

In this project, a nano-composite based on graphitized carbon nitride and its derivatives was fabricated, and its physical and chemical properties were studied to evaluate its performance in targeted applications. The results demonstrated that the nano-composite exhibits remarkable absorption and surface interaction properties, making it a promising material for various applications such as photocatalysis, pollutant treatment, and electronic devices.

References:

.1 F. Dong, et al. Efficient synthesis of polymeric gC 3 N 4 layered materials as novel efficient visible light driven photocatalysts. *Journal of Materials Chemistry* 2011; 21:15171-15174..

.2 F. Goettmann, A. Fischer, M. Antonietti, and A. Thomas. Metal-free catalysis of sustainable Friedel–Crafts reactions: direct activation of benzene by carbon nitrides to avoid the use of metal chlorides and halogenated compounds. *Chemical communications* 2006; 4530-4532..

.3 W.-J. Ong, et al. Graphitic carbon nitride) g-C3N4)-based photocatalysts for artificial photosynthesis and environmental remediation: are we a step closer to achieving sustainability? *Chemical reviews* 2016; 116:7159-7329..

.4 X. Liu, et al. Recent developments of doped g-C3N4 photocatalysts for the degradation of organic pollutants. *Critical Reviews in Environmental Science and Technology* 2021; 51:751-790..

.5 M.M. Taha, L.G. Ghanem, M.A. Hamza, and N.K. Allam. Highly stable supercapacitor devices based on three-dimensional bioderived carbon encapsulated g-C3N4 nanosheets. *ACS Applied Energy Materials* 2021; 4:10344-10355..

.6 L. Ge, C. Han, J. Liu, and Y. Li. Enhanced visible light photocatalytic activity of novel polymeric g-C3N4 loaded with Ag nanoparticles. *Applied Catalysis A: General* 2011; 409..222-215:

.7 A. Alaghmandfard and K. Ghandi. A comprehensive review of graphitic carbon nitride (g-C3N4)–metal oxide-based nanocomposites: potential for photocatalysis and sensing. *Nanomaterials* 2022; 12:294..

.8 J.N. Tiwari, R.N. Tiwari, and K.S. Kim. Zero-dimensional, one-dimensional, two-dimensional and three-dimensional nanostructured materials for advanced electrochemical energy devices. *Progress in Materials Science* 2012; 57:724-803..

.9 E.C. Dreaden, et al. The golden age: gold nanoparticles for biomedicine. *Chemical Society Reviews* 2012; 41:2740-2779..

.10 W.-K. Shin, et al. Cross-linked composite gel polymer electrolyte using mesoporous methacrylate-functionalized SiO2 nanoparticles for lithium-ion polymer batteries. *Scientific reports* 2016; 6:2..6332

.11 J.E. Lee, et al. Multifunctional mesoporous silica nanocomposite nanoparticles for theranostic applications. *Accounts of chemical research* 2011; 44:893-902..

.12 M. Mansha, et al. Synthesis of In2O3/graphene heterostructure and their hydrogen gas sensing properties. *Ceramics International* 2016; 42:11490-11495..

.13 I. Rawal and A. Kaur. Synthesis of mesoporous polypyrrole nanowires/nanoparticles for ammonia gas sensing application. *Sensors and Actuators A: Physical* 2013; 203:92-102..

.14 S. Ali ,et al. Electrocatalytic performance of Ni@ Pt core–shell nanoparticles supported on carbon nanotubes for methanol oxidation reaction. *Journal of Electroanalytical Chemistry* 2017; 795:17-25..

.15 S. Afolalu, et al. *Morphological characterization and physio-chemical properties of nanoparticle-review*. in *IOP Conference Series: Materials Science and Engineering*. 2019. IOP Publishing..

.16 M. Ganesh, P. Hemalatha, M.M. Peng, and H.T. Jang. One pot synthesized Li, Zr doped porous silica nanoparticle for low temperature CO2 adsorption. *Arabian Journal of Chemistry* 2017; 10:S1501-S1505..

.17 P. Ramacharyulu, et al. Iron phthalocyanine modified mesoporous titania nanoparticles for photocatalytic activity and CO 2 capture applications. *Physical Chemistry Chemical Physics* 2015; 17:26456-26462..
.18 M. Shaalan, M. Saleh, M. El-Mahdy, and M. El-Matbouli. Recent progress in applications of nanoparticles in fish medicine: a review. *Nanomedicine: Nanotechnology, Biology and Medicine* 2016; 12:701-710..
.19 L.F. Mabena ,S. Sinha Ray, S.D. Mhlanga, and N.J. Coville. Nitrogen-doped carbon nanotubes as a metal catalyst support. *Applied Nanoscience* 2011; 1:67-77..
.20 I. Gessner and S. Mathur. Dual function nanoconjugates for biomedical imaging and targeted drug delivery. *Nanotechnologies in Preventive and Regenerative Medicine; Uskovic, V., Ed.; Elsevier Ltd.: Oxford, UK* 2018; 260-297..
.21 C.M. Huber, et al. A Review on Ultrasound-based Methods to Image the Distribution of Magnetic Nanoparticles in Biomedical Applications .*Ultrasound in Medicine & Biology* 2024. ;
.22 M. Tadic, M. Panjan, V. Damnjanovic, and I. Milosevic. Magnetic properties of hematite (α-Fe2O3) nanoparticles prepared by hydrothermal synthesis method. *Applied Surface Science* 2014; 320:183-187..
.23 P. Dash ,S. Raut, M. Jena, and B. Nayak. Harnessing the biomedical properties of ferromagnetic α-Fe2O3 NPs with a plausible formation mechanism. *Ceramics International* 2020; 46:26190-26204..
.24 M.N. Chong, B. Jin, C.W. Chow, and C. Saint. Recent developments in photocatalytic water treatment technology: a review. *Water research* 2010; 44:2997-3027..
.25 F. Sudarman, M. Shiddiq, B. Armynah, and D. Tahir. Silver nanoparticles (AgNPs) synthesis methods as heavy-metal sensors: A review. *International Journal of Environmental Science and Technology* 2023; 20:9351-9368..
.26 S. Some, et al. Biosynthesis of silver nanoparticles and their versatile antimicrobial properties. *Materials Research Express* 2018; 6:012001..
.27 T. Bruna, F. Maldonado-Bravo, P. Jara, and N. Caro .Silver nanoparticles and their antibacterial applications. *International journal of molecular sciences* 2021; 22:7202..
.28 F. Rodríguez-Félix, et al. Trends in Sustainable Green Synthesis of Silver Nanoparticles Using Agri-Food Waste Extracts and Their Applications in Health. *Journal of Nanomaterials* 2022; 2022:8874003..
.29 R. Katwal, et al. Electrochemical synthesized copper oxide nanoparticles for enhanced photocatalytic and antimicrobial activity. *Journal of Industrial and Engineering Chemistry* 2015..184-31:173 ;
.30 Q. Zhang, et al. CuO nanostructures: synthesis, characterization, growth mechanisms, fundamental properties, and applications. *Progress in Materials Science* 2014; 60:208-337..
.31 M. Khatri, et al. Evaluation of cytotoxic, genotoxic and inflammatory responses of nanoparticles from photocopiers in three human cell lines. *Particle and fibre toxicology* 2013; 10:1-22..
.32 J.S. Kim, et al. Effects of copper nanoparticle exposure on host defense in a murine pulmonary infection model. *Particle and fibre toxicology* 2011; 8:1-14..
.33 V. Aruoja, H.-C. Dubourguier, K. Kasemets, and A. Kahru. Toxicity of nanoparticles of CuO, ZnO and TiO2 to microalgae Pseudokirchneriella subcapitata. *Science of the total environment* 2009; 407:1461-1468..
.34 M .Sahooli, S. Sabbaghi, and R. Saboori. Synthesis and characterization of mono sized CuO nanoparticles. *Materials Letters* 2012; 81:169-172..
.35 K.S. Khashan, G.M. Sulaiman, and F.A. Abdulameer. Synthesis and antibacterial activity of CuO nanoparticles suspension induced by laser ablation in liquid. *Arabian journal for science and Engineering* 2016; 41:301-310..

.36 M. Ahamed, et al. Genotoxic potential of copper oxide nanoparticles in human lung epithelial cells. *Biochemical and biophysical research communications* 2010; 396:578-583..
.37 M. Mortimer, K. Kasemets, and A. Kahru. Toxicity of ZnO and CuO nanoparticles to ciliated protozoa Tetrahymena thermophila. *Toxicology* 2010; 269:182-189..
.38 M.K. Mohammed. Synthesis and Characterization of α-Fe2O3 Nanoparticles Using the Precipitation and Eco-Friendly Methods. *Journal of Pharmaceutical Negative Results* 2022; 13:782-789..
.39 M. Muhi. Preparation of silver nanoparticles by chemical reaction method at different reaction temperatures and the study of their antibacterial activity. *Engineering and Technology Journal* 2017; 35.:
.40 K. Phiwdang, S. Suphankij, W. Mekprasart, and W. Pecharapa. Synthesis of CuO nanoparticles by precipitation method using different precursors. *Energy procedia* 2013; 34:740-745..
.41 A.A. Alshahrani, et al. The preparation of Zr-TiO2@ g-C3N4 nanocomposites to remove ciprofloxacin from water. *Journal of Molecular Structure* 2024; 138891..
.42 S. Naz, et al. Green synthesis of hematite (α-Fe2O3) nanoparticles using Rhus punjabensis extract and their biomedical prospect in pathogenic diseases and cancer. *Journal of Molecular Structure* 2019; 1185:1-7..
.43 A.A. Radhakrishnan and B.B. Beena. Structural and optical absorption analysis of CuO nanoparticles. *Indian J. Adv. Chem. Sci* 2014; 2:15..161-8
.44 R. Agha Beygli, N. Mohaghegh, and E. Rahimi. Metal ion adsorption from wastewater by gC 3 N 4 modified with hydroxyapatite: a case study from Sarcheshmeh Acid Mine Drainage. *Research on Chemical Intermediates* 2019; 45:2255-2268..
.45 Z. Alhalili. Green synthesis of copper oxide nanoparticles CuO NPs from Eucalyptus Globoulus leaf extract: Adsorption and design of experiments. *Arabian Journal of Chemistry* 2022; 15:103739..
.46 P.K. Raul, et al. CuO nanorods: a potential and efficient adsorbent in water purification. *Rsc Advances* 2014; 4:40580-40587..
.47 M. Khan, et al. Search for effective approaches to fight microorganisms causing high losses in agriculture: application of P. lilacinum metabolites and mycosynthesised silver nanoparticles. *Biomolecules* 2022; 12:174..
.48 P. Kubelka and F. Munk. A contribution to the optics of pigments. *Z. Tech. Phys* 1931; 12:193..
.49 P. Makuła, M. Pacia, and W. Macyk, *How to correctly determine the band gap energy of modified semiconductor photocatalysts based on UV–Vis spectra*. 2018, ACS Publications. p. 6814-6817..